7V European Conference on Computational Fluid Dynamics
ECCOMAS CFD 2010
J. C. F. Pereira and A. Sequeira (Eds)
Lisbon, Portugal, 14–17 June 2010

BOUSS3W NONLINEAR WAVE PROPAGATION MODEL. BOTTOM FRICTION IMPLEMENTATION

Pinheiro L.V.[*], Fortes C. J.[*], Teixeira P.R.[†], Walkley M.A.[‡]

[*]National Laboratory for Civil Engineering
Av. Brasil 101, 1700-066 Lisbon
e-mail: lpinheiro@lnec.pt; jfortes@lnec.pt

[†]Federal University of Rio Grande
Escola de Engenharia, Av. Itália, km8, Campus Carreiros, 96201-900 Rio Grande, RS, Brasil
e-mail: pauloteixeira@furg.br

[‡]University of Leeds
School of Computing, University of Leeds, Leeds, LS2 9JT
e-mail: m.a.walkley@leeds.ac.uk

Key words: Wave propagation, Bottom friction, Finite element.

Abstract. *This paper describes the implementation of bottom friction and wave breaking physical processes in the BOUSS3W model. BOUSS3W is a finite element numerical model for wave propagation in near shore regions and wave penetration in harbours and sheltered zones. The extended Boussinesq equations derived by Nwogu (1993) are solved. These equations describe the nonlinear evolution of waves over a sloping impermeable bottom and are able to reproduce some of the most important physical effects associated with the nonlinear wave transformation in near shore regions. Their range of validity extends from shallow up to intermediate water depths. Both regular and irregular waves can be generated.*

Previous applications of the model confirm that the model is able to simulate quite well the main characteristics of the wave field outside and inside harbour configurations. However, neither bottom friction nor wave breaking phenomena were included in the model. These two phenomena constitute an important form of energy dissipation that cannot be neglected in near shore areas.

This paper presents a general description of BOUSS3W and its newest developments, namely, bottom friction and wave breaking. Then, the application of the numerical model to simple test cases as well to a real case is described.

1 INTRODUCTION

The most important physical effects associated with the nonlinear wave transformation of waves in nearshore regions can be described by Boussinesq-type equations (Kirby (1997)). One example of this class of equations was introduced by Nwogu (1993). These equations describe the nonlinear evolution of waves over a sloping impermeable bottom without considering wave breaking. Their range of validity extends from shallow up to intermediate water depths where the nonlinear and dispersive effects are mild. Therefore, they seem adequate to describe the wave field outside and inside ports, harbours and sheltered zones. In the last few decades several authors have been working to extend the applicability domain of these equations to deep as well as very shallow waters and also to include other physical phenomena such as currents, wave breaking, bottom friction, etc… Nowadays there is a large family of extended Boussinesq equations (Madsen *et al.* 1991, 2002, 2006; Beji and Nadaoka 1996; Nwogu 1993; Wei *et al.* 1995b; Gobbi and Kirby 1996; Madsen and Schäffer 1998a, 1998b; Agnon *et al.* 1999; Zou 2000; Kennedy *et al.* 2000).

The numerical resolution of Boussinesq-type equations have mostly used finite diference methods (Peregrine 1967; Madsen *et al.* 1991; Madsen e Sørensen 1992; Beji and Battjes 1994; Wei and Kirby 1995; Kirby *et al.* 1998 and Lynett 2002). But, although computationally more complex, the finite element method deals directly with unstructured grids that correctly represent the physical boundaries of the domain, including the coastline, islands and other obstacles. Moreover the finite element method allows minimizing the number of points in the grid using local refinement techniques. Several authors have used this method with success (Katapodes e Wu 1987; Ambrosi 1997; Grasselli *et al.* 1997; Antunes do Carmo and Seabra Santos 1996; Li *et al.* 1999; Walkley 1999; Walkley and Berzins 1999; 2002). These models use different time integration schemes and either triangular or rectangular linear elements. Recent advances in computational resources allow for inclusion of higher levels of non-linear and frequency dispersion terms as well as more complex interpolation functions (Woo and Liu 2001 and Eskilsson *et al.* 2006).

Developments on the Walkey's model (Walkley 1999; Walkley and Berzins 1999; 2002) led to BOUSS3W model, which includes internal wave generation (using the source function method with which regular and irregular waves can be generated), artificial numerical viscosity (to control numerical instabilities) and numerical sponge layers (placed on radiation boundaries to absorb outgoing waves) and numerical porosity layers (placed whether on physical boundaries or inside the domain to simulate the reflection, transmission and energy dissipation effects of porous structures on the waves).

In the following section, the governing equations are summarized. The boundary conditions and the source function methods are also discussed. Numerical examples to validate the model are given. The numerical results are compared with results from other numerical models, demonstrating the main advantages and limitations of using this model in real life case studies.

2 BOUSS3W NUMERICAL MODEL

2.1 Model description

The extended Boussinesq equations derived by Nwogu (1993) are given by the following equations, at depth $Z_\alpha = \theta h$.

$$\frac{\partial \eta}{\partial t} + \nabla((h+\eta)\mathbf{u}) + \nabla \cdot \left(\left(\frac{Z_\alpha{}^2}{2} - \frac{h^2}{6} \right) h \nabla(\nabla \cdot \mathbf{u}) + \left(Z_\alpha + \frac{h}{2} \right) h \nabla(\nabla \cdot (h\mathbf{u})) \right) = 0 \tag{1}$$

$$\frac{\partial \mathbf{u}}{\partial t} + (\mathbf{u} \cdot \nabla)\mathbf{u} + g \nabla \eta + \frac{Z_\alpha{}^2}{2} \nabla \left(\nabla \cdot \frac{\partial \mathbf{u}}{\partial t} \right) + Z_\alpha \nabla \left(\nabla \cdot \left(h \frac{\partial \mathbf{u}}{\partial t} \right) \right) = 0 \tag{2}$$

where η is the free surface elevation, $\mathbf{u} = \mathbf{u}(x, y, t) = (\mathrm{u}, \mathrm{v})$ is the velocity vector, h the water depth.

The original Nwogu's equations were further extended to take into account some important physical processes (wave transmission through porous structures, bottom friction and wave breaking) as well as other source/damping terms for numerical reasons. The BOUSS3W model equations result as follows:

$$\frac{\partial \eta}{\partial t} + \nabla((h+\eta)\mathbf{u}) + \nabla \cdot \left(\left(\frac{Z_\alpha{}^2}{2} - \frac{h^2}{6} \right) h \nabla(\nabla \cdot \mathbf{u}) + \left(Z_\alpha + \frac{h}{2} \right) h \nabla(\nabla \cdot (h\mathbf{u})) \right) = S_f + (\upsilon_t + \upsilon_s)\nabla^2 \eta \tag{3}$$

$$\frac{\partial \mathbf{u}}{\partial t} + (\mathbf{u} \cdot \nabla)\mathbf{u} + g \nabla \eta + \frac{Z_\alpha{}^2}{2} \nabla \left(\nabla \cdot \frac{\partial \mathbf{u}}{\partial t} \right) + Z_\alpha \nabla \left(\nabla \cdot \left(h \frac{\partial \mathbf{u}}{\partial t} \right) \right) = n\mathbf{u}\left(f_l + n f_t |\mathbf{u}|\right) + \frac{1}{h+\eta}\left(f_w \mathbf{u}|\mathbf{u}| + \nabla \upsilon_e \nabla (h+\eta)\mathbf{u}\right) \tag{4}$$

where S_f is a source function, $(\upsilon_t + \upsilon_s)\nabla^2 \eta$ is a viscous damping term, $n f_l \mathbf{u} + n f_t \mathbf{u}|\mathbf{u}|$ are laminar and turbulent friction terms, $\frac{1}{h+\eta} f_w \mathbf{u}|\mathbf{u}|$ is a wave induced bottom friction term and $\frac{1}{h+\eta} \nabla \upsilon_e \nabla (h+\eta)\mathbf{u}$ is the wave breaking term. These additional terms are detailed in the following sections.

2.1.1. Source function

It is possible to specify incident wave conditions at the entrance boundary, but the characteristics of reflected waves in the computational domain cannot be determined *a priori*. This poses a problem when using complex geometries and long term simulations. Walkley's (1999) solution to solve the issue of reflected waves inside the domain returning to the generation region was based upon a time varying sea bed. This method lacked a rigorous derivation and was difficult to extend to irregular waves, since no mathematical relation between wave amplitude and seabed elevation was established.

Wei *et al.* (1999) presented a similar method to that of Walkley (1999) but, instead, introduced a source function term ($S_f(x,t)$, equation (5)) in the mass balance equation.

$$S_f(x,t) = D \cdot e^{\left(-\sigma \cdot (x_s - x)^2\right)} \cdot \sin(-\omega \cdot t) \tag{5}$$

where D is the amplitude of the source function, σ is a parameter corresponding to the width of the source region and x_s is the centre of the source region. In their calculations an assumption was made that the nonlinear effects are small in the narrow source region. A linearization of the Boussinesq equation is made and by using Green's theorem, and an analytical relation between source function amplitude and wave amplitude is obtained, equation (6).

$$D = 2 \cdot \eta_0 \cdot \frac{\left(\omega^2 - \alpha_1 \cdot g \cdot k^4 \cdot h^3\right)}{\omega \cdot I_1 \cdot k \cdot \left(1 - \alpha (kh)^2\right)} \tag{6}$$

where $\alpha_1 = \alpha + 1/3$, and I_1 is given by equation (7).

$$I_1 = \sqrt{\frac{\pi}{\sigma}} \cdot e^{\left(-\frac{k^2}{4\sigma}\right)} \tag{7}$$

The σ parameter is defined in order to get the desired width, *W*, for the source function. The source function width is given in terms of half wavelength, equation (8).

$$W = \delta \cdot \frac{L}{2} \tag{8}$$

Hence σ is given by equation (9).

$$\sigma = \frac{80}{\delta^2 L^2} \tag{9}$$

The source function will have maximum amplitude equal to *D* and a width equal to *W*.

2.1.2. Viscous damping

A viscous term (ν_s) was added to the the free surface equation .This viscous term grows quadratically in the part of the domain corresponding to the sponge layer, equation (31), see Figure 1: .

$$\nu_s = \nu_2 \cdot \frac{e^{\left(\frac{x - x_s}{x_F - x_s}\right)^2} - 1}{e - 1} + \nu_1 \tag{10}$$

$$\nu_2 = \frac{30}{T} \tag{11}$$

where, ν_1 is the viscosity used throughout the domain to control the numerical instabilities, and ν_2 is the maximum viscosity at the sponge layer.

It was found in practice that the width of the sponge layer must be one to two wavelengths, in order to provide sufficient damping, Kirby et al. 1998.

2.1.3. Porous structures

The modified equations for the porous region are obtained by replacing *u* with *u*/*n*, where *n* is the porosity, and including a term to account for energy dissipation inside the structure:

$$F_p = n\, f_l\, \mathbf{u} + n\, f_t\, \mathbf{u}|\mathbf{u}| \tag{12}$$

where f_l and f_t are laminar and turbulent friction factors, respectively. These factors are obtained using the empirical relationships recommended by Engelund (1953):

$$f_l = \alpha_0 \frac{(1-n)^3}{n^2} \frac{\upsilon}{d^2} \tag{13}$$

$$f_t = \beta_0 \frac{(1-n)}{n^3} \frac{1}{d^2} \tag{14}$$

where υ is the kinematic viscosity of water, *d* is the characteristic stone size, and α_0 and β_0 are empirical constants that range from 780 to 1500, and from 1.8 to 3.6 respectively. The characteristic stone size is given by:

$$d = \left(\frac{W_s}{g \cdot \rho_s} \right)^{1/3} \tag{15}$$

where W_s is the stone weight in kN and ρ_s is the mass density of armor material (2.65 kg/m^3 for quarrystone and 2.3 kg/m^3 for concrete blocks).

However, porosity layers, as well as viscosity layers, also must be introduced gradually to avoid large discontinuities which lead to instability. So, a Gaussian function is used to distribute growing porosity in half a wavelength width. Figure 1: shows an example of varying viscosity and porosity.

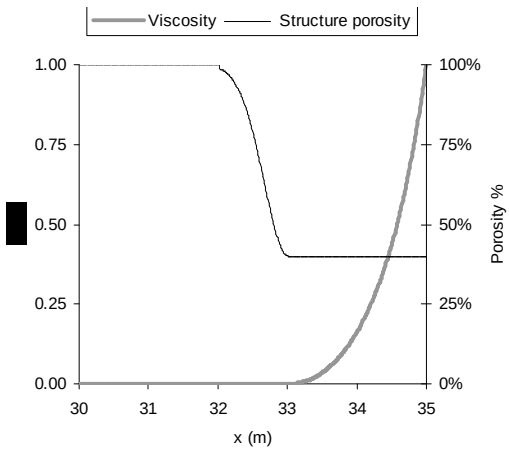

Figure 1: Viscosity (quadratic growth in sponge layer) and Porosity (Gaussian growth in porous layer).

2.2 Boundary conditions

The boundary conditions can be of three types: full reflection, full absorption or partial reflection.

2.2.1. Full reflection condition

Solid boundaries can fully or partially reflect incident waves. Full reflection represents a solid impermeable vertical wall. Non permeability and mass conservation conditions lead to the following boundary conditions:

$$\mathrm{u} \cdot \mathrm{n} = 0 \text{ and } \mathrm{w} \cdot \mathrm{n} = 0 \tag{16}$$

Where n is perpendicular to the boundary.

2.2.2. Full absorption condition - Sponge layers

It is important to fully absorb all incident waves at the outgoing boundaries. Due to the dispersive nature of the equations modeled, a simple radiation boundary condition is not completely effective, as the dispersive waves have no single phase speed. Therefore, a viscous damping layer, termed sponge layer, is introduced near the outflow boundary in order to absorb incident waves at those boundaries. These sponge layers take the form of:

$$SL = \upsilon_s \nabla^2 \eta \tag{17}$$

2.2.3. Partial reflection condition – Porous layers

To partially absorb wave energy at a given boundary the sponge layer can be tuned to do so, as described in Nwogu and Dermirbilek (2001). However, this method is not linear, so further investigation must be done to determine a mathematical expression that correlates the reflection coefficient to the amount of viscosity and to the width of the sponge layer.

Another method, also presented by Nwogu and Dermirbilek (2001) is to modify the Boussinesq equations to simulate partial wave reflection and transmission through porous structures such as breakwaters.

2.3 Time integration

The solution of the differential-algebraic system is carried out by the DASPK package (Brown et al 1989). Sparse matrices are preconditioned using incomplete lower-upper (ILU) factorisations of the original matrix, which reduces the computational time and storage requirements of the full LU factorisation by disregarding a certain amount of the fill-in entries based on numerical tolerances. The DASPK software contains routines from the SPARSKIT package (Saad 1996) for the iterative solution of large sparse equation systems with the method GMRES. Absolute and relative errors are controlled using variable step size and order. It was determined, after some trials, that the relative (*rtol*) and absolute (*atol*) tolerances should be set to $rtol=atol=10^{-6}$.

2.4 Initial conditions

Initial conditions for this problem are those for an undisturbed free surface. For this initial condition, as the wave enters the domain, the integration software will identify that as a discontinuity, forcing the use of very small time steps. In order to avoid this, a smoothing function (v_t) is introduced:

$$v_t = m_1 \cdot e^{-m_2 \frac{t}{T}} \tag{18}$$

where T is the wave period and m_1 and m_2 are constants that must be determined experimentally. This term is added to the free surface equation as a viscous coefficient. In the first time steps this will damp the solution, allowing the use of larger time steps. Due to the exponential decay nature of this damping term, it will not affect the solution obtained after a suitably large time.

2.5 Inputs and outputs

For a friendly use of the numerical model BOUSS3W a Graphical User Interface (GUI) was developed in Microsoft Excel™ Environment using Visual Basic for Applications™ (VBA) as the programming language. This GUI builds all the data files and executes the model. The inputs needed for a correct use of the model are:

- Wave characteristics: period, wave height and tide level, or time series of surface elevation;
- Mesh characteristics: nodes, elements, depths and boundary conditions;
- Time integration parameters;
- Numerical diffusion parameters;
- Output parameters.

The finite element mesh is created using the mesh generator, GMALHA, Pinheiro *et al.* (2007a). This mesh generator produces unstructured triangular finite element mesh with optimized node density according to local wavelength, optimized element geometry and minimized bandwidth with the Reverse Cuthill McKee method (Cuthill and McKee 1969).

The model produces several types of outputs, such as:

- Plots of surface elevation;
- Plots of velocities;
- Plots of wave height index;
- Time series of surface elevation at given points.

3 BOTTOM FRICTION

The bottom boundary layer of flow associated with the passage of waves is normally restricted to a small region above the sea floor, unlike river and tide flows where it stretches all the way till the free surface. There is therefore a very small amount of energy dissipation due to bottom friction in typical wave propagation distances of the order of 1km used in Boussinesq-type models. The energy dissipation due to bottom friction, however plays an important role in the wave transformations near shore, in very shallow waters, Jonhson and Kofoed-Hansen (2000).

The effect of energy dissipation due to a turbulent bottom boundary layer is simulated using a term of bottom shear stress, F_b, to the momentum equation, following the procedure adopted by Nwogu and Demirbilek (2001).

$$F_b = \frac{1}{h+\eta} f_w U_\alpha |U_\alpha| \quad (19)$$

where f_w is the wave friction factor. This equation is expressed in terms of $U\alpha$ instead of the bottom velocity in order to minimize the computational effort to detrmine it.

The wave friction factor estimates the bottom shear stress induced by the passage of the wave. Many authors have tried to estimate this factor (Jonsson, 1963; Jonsson, 1965; Jonsson, 1966; Schlichting, 1968; Komar and Miller, 1973; Swart, 1974) but normally their approach depends on a number of variables, sometimes very hard to estimate. The wave friction factor evaluated with all these different approaches can differ by a factor of 3.

In the BOUSS3W model two approaches are made available. The first one is very expedite and is related solely to the Chezy coefficient (C_f):

$$f_w = \frac{g}{C_f^{\,2}} \quad (20)$$

In Figure 2: a method of evaluating the Chezy coefficient according to the type of sea bed and water depth is presented, Soulsby (1997). In Figure 3: the variation of the wave friction factor with the Chezy number.

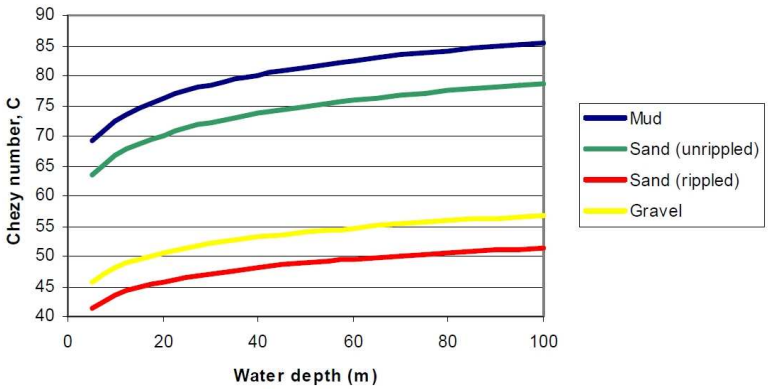

Figure 2: Variation of Chezy numbers from Soulsby (1997). Adapted from Lambkin (2010).

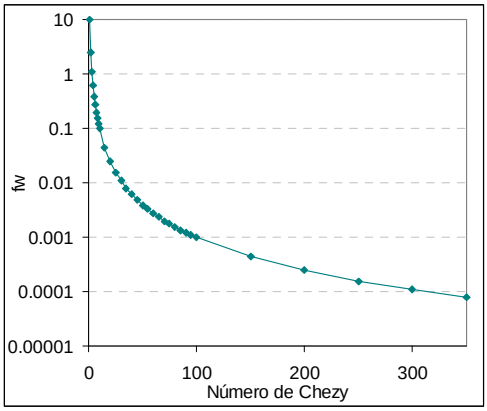

Figure 3: Variation of the wave friction factor with Chezy numbers.

The other way of estimating the wave friction factor included in the model is the method presented by Leroux (2003). This author proposes a rigorous form of expressing f_w using solely two variables, the equivalent diameter of the particles, D, and the wave period, T.

$$f_w = \frac{2\beta g \rho_\gamma D}{U_{wcr}^2 \rho} \tag{21}$$

where ρ_γ e ρ are the densities of the submerged particles and of water, respectively. The Shields parameter, β, is given by:

$$\beta = \begin{cases} -0.0717\log(W_{ds}) + 0.0625 & \Leftarrow W_{ds} < 2.5 \\ 0.0717\log(W_{ds}) + 0.0272 & \Leftarrow 2.5 < W_{ds} < 11 \\ 0.045 & \Leftarrow W_{ds} > 11 \end{cases} \tag{22}$$

The critical orbital velocity, U_{wcr} is given by:

$$U_{wcr} = -0.002\left(\left(\theta_{wcr} g D \rho_\gamma\right)^2 \frac{T}{\rho\mu}\right) + 1.0702\left(\theta_{wcr} g D \rho_\gamma \left(\frac{T}{\rho\mu}\right)^{0.5}\right) \tag{23}$$

with $\theta_{wcr} = 0.027 W_{ds}^{-0.6757}$, where W_{ds} is the nondimensinal sedimentation velocity and can be evaluated according to the empirical formulation of Dietrich (1982):

$$W_{ds} = 0.68\frac{D^2}{5832} \tag{24}$$

In Figure 4: the variation of the wave friction factor with the equivalent diameter of the particles, *D*, and the wave period, *T*, is presented using the procedure of LeRoux (2003), considering the particles density of $2.65 \times 10^3 kgm^{-3}$.

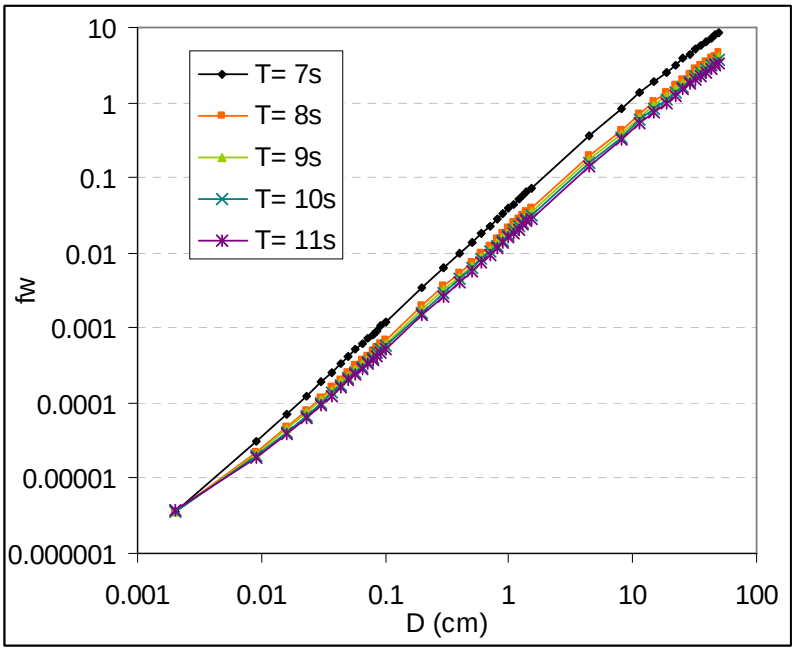

Figure 4: Variation of the wave friction factor with *D* and *T*, using LeRoux´s method (2003).

4 APPLICATIONS

The numerical model was applied to the simulation of regular wave propagation over a constant depth flume and to a real test case: Faro beach. All numerical calculations were done on a workstation LINUX CORVUS with four processors AMD Opteron™ 265, 2GHz, 8GB RAM memory.

4.1 A constant slope bottom 2D-Channel

To validate the bottom friction implementation BOUSS3W was run in a simple test case of a flat bottom 2D-Channel. The wave friction factor effect was investigated.

4.1.1. Numerical conditions

The channel is 35 m long, 2 m wide and has a water depth of 0.4 m, Figure 5: . A regular wave of 0.01 m of amplitude and 2.0 s period was generated at x = 8 m. The wave length is of 3.7 m. The domain was discretized with 10428 triangular finite elements containing 5511 points. The bandwidth of the mesh is of 34.

Two sponge layers were placed at each end of the flume with 2 m length each. Two sets of values were tested for the wave friction factor, Table 1. The simulation time was of 60s.

Table 1 Wave friction factors tested.

chezy	fw	chezy	fw
1	9.81	15	0.0436
2	2.45	25	0.0157
3	1.09	35	0.0080
4	0.61	45	0.0048

5	0.39	55	0.0032
6	0.27	65	0.0023
7	0.20	75	0.0017
8	0.15	85	0.0014
9	0.12	95	0.0011
10	0.10	105	0.0009

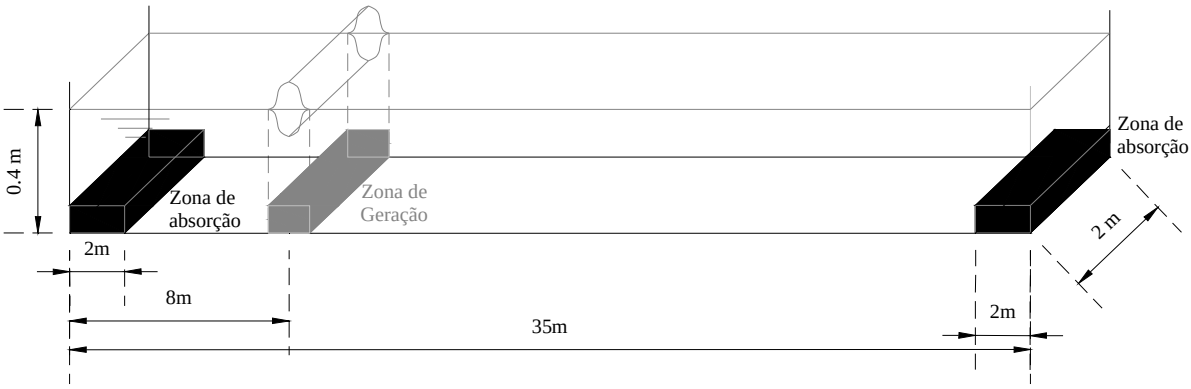

Figure 5: Flat bottom 2D-channel.

4.1.2. Results

In Figure 6: , the reduction of the wave amplitude is presented in percentage for each of the wave friction factors values tested.

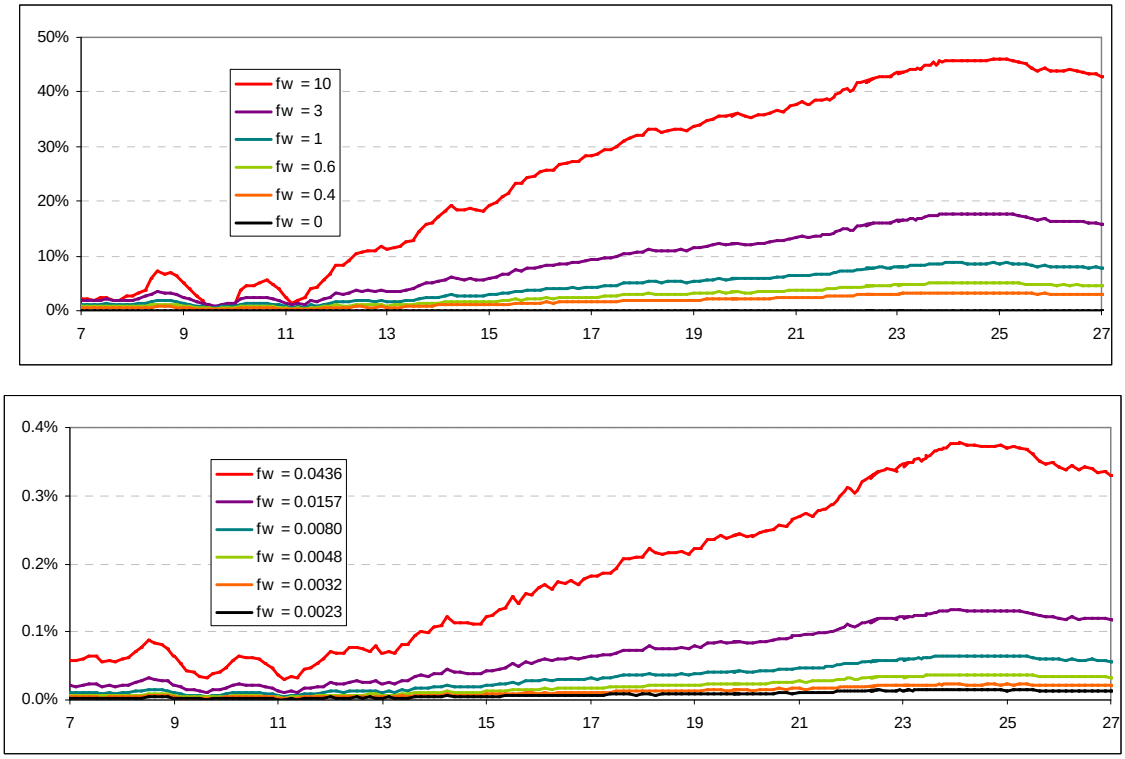

Figure 6: Reduction of the wave amplitude.

In the first set of *fw* values, the reduction of the wave energy is clear and grows as the wave propagates reaching as high as a factor of 45% for fw=10.

In the second set of *fw* values, the reduction of the wave energy is very faint but still the tendency is consistent with the magnitude of the wave friction factor.

In Figure 7: the maximum reduction of the wave height, at x≈25m (right before the sponge layer takes effect on absorbing the wave) is presented.

These results confirm the adequate implementation of the bottom friction in the model, as the energy dissipation behaves like expected with the variation of the wave friction factor.

The implementation of this new physical phenomenon does not introduce any instabilities in the model and the viscous damping term was not necessary in any simulation.

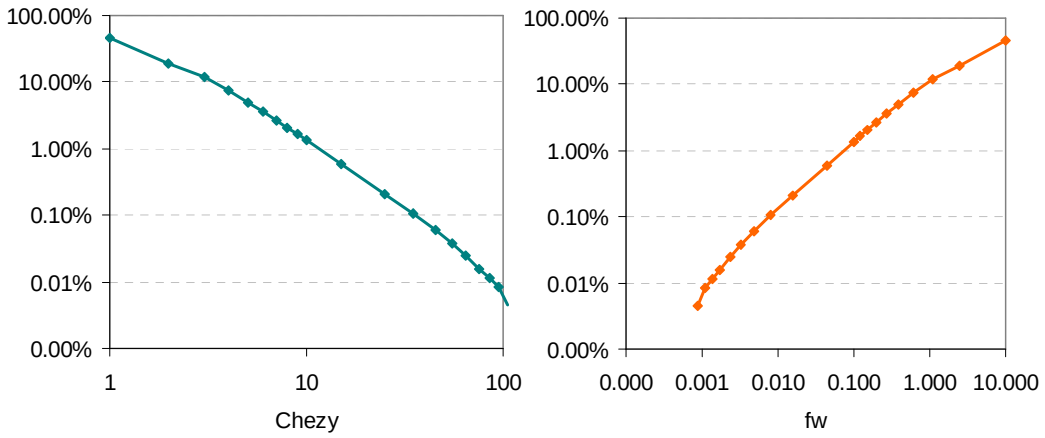

Figure 7: Maximum reduction (at x≈25m) of the wave height.

4.2 Real test case - Faro Beach

Faro beach, also known as “island of Faro”, is located in the Ancão peninsula which delimitates the Ria Formosa lagoon to the west. This beach is art of the Faro municipality in the Algarve region.

Faro beach is a sandy beach which extends for several kilometers, Figure 8

Figure 8: Faro Beach.

The area is characterized by a more or less regular bathymetry parallel to the shore. Two topographic surveys, obtained in the scope of the BRISA project, were used to characterize the bathymetry of the study area, **Error! Reference source not found.**.

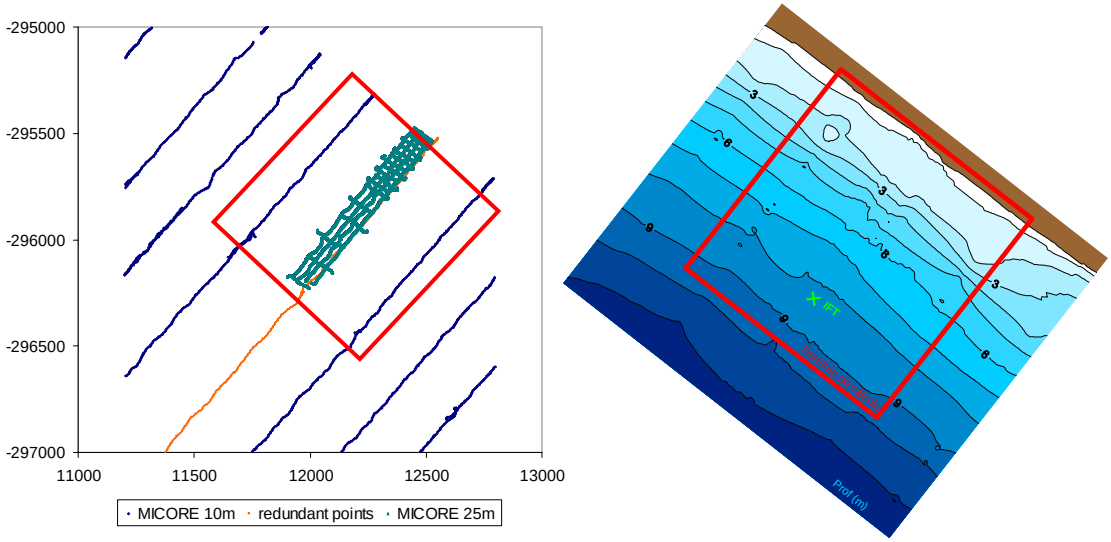

Figure 9: a) Bathymetryc surveys; b) Interpolated bathymetry, numerical domain and pressure sensor *Infinity* location (IFT).

The wave climate offshore of the Faro beach is characterized by significant wave heights between 0.14 m and 4.4 m, being more frequent between 0.5 m and 1.0 m; periods between 3.0 s and 10.7 s, being more frequent between 3.0 s and 4.0 s and the average directions between 0º and 340º, being more frequent between 250º and 270º. These data were collected at a wave buoy deployed near the area between 1986 and 1995, Raposeiro *et al.* (2009).

4.2.1. Methodology

In this real test case, the performance of the model is evaluated with the new physical phenomenon introduced. For this model results are compared with another Boussinesq-type model, COULWAVE, Lynett (2002). This model is based upon the extended Boussinesq equations derived by Wei *et al.*, 1995. It also includes bottom friction and has been previously tested successfully, making it a good comparison tool.

For the numerical runs of BOUSS3W the following steps are necessary:

- Definition of the numerical domain:
- Construction of a finite element mesh optimized regarding local depths, using GMALHA mesh generator;
- Generation of regular waves.

The analysis of the results includes:

- Free surface elevations in all points of the domain for certain time steps
- Time series of free surface elevations in designated points of the domain.

4.2.2. Numerical conditions

Regular waves of 0.3 m of amplitude, 8 s period and wave direction of S37ºW (217º). The tide level was of +2.0 m (Z.H.).

The numerical domain was discretized with a triangular finite element mesh containing 110 828 nodes and 220 470 elements. In average, the mesh contains 22 points per wave length considering a period of 8 s. The bandwidth is of 509.

In Figure 10: the numerical domain is depicted including the generation line and the sponge layers two wave lengths (132 m) wide each.

The time step was of 0.1 s. A viscous damping factor of 7.0×10^{-6} m^2/s was used. The simulation time was of 200 s. The wave friction factor was of fw=0.0023.

Six points were defined for results analysis, Table 2.

Table 2: Loaction of points.

Point	Real Coordinates		Mesh Coordinates	
	X	Y	X	Y
P1	12342.17	-296305.18	425	150
P2	12434.03	-296186.60	425	300
P3	12556.52	-296028.49	425	500
P4	12679.01	-295870.39	425	700
P5	12511.02	-295740.25	212.5	700
P6	12846.99	-296000.53	637.5	700

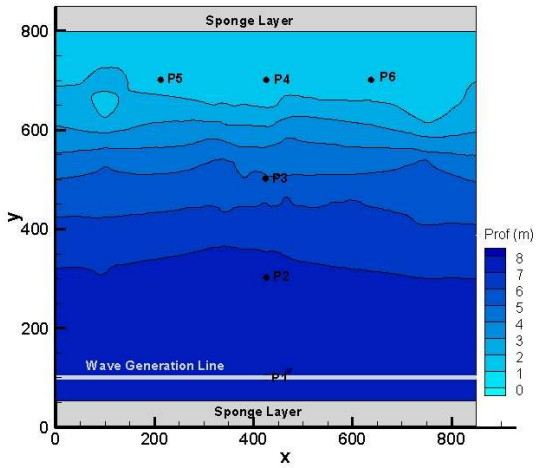

Figure 10: Location of generation line, sponge layers and points P1 to P6

4.2.3. Results

In Figure 11: the results of the free surface elevation at 200 s and the wave height indexes (H/H0) are presented as well as a 3D view of the free surface elevation at 200 s. This shows the wave transformations and interactions with the bottom along the beach slope as the wave propagates.

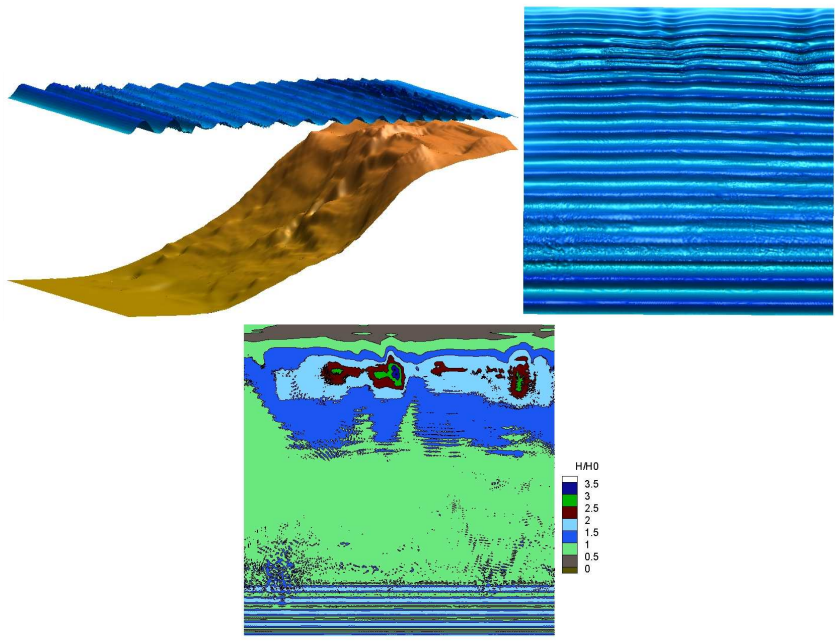

Figure 11: Free surface elevation (3D and 2D views) and wave height indexes at time instant t = 200 s.

Figure 12 presents the free surface elevation at the six points with the two models BOUSS3W and COULWAVE.

In general, both models reproduce well the wave transformations. Both reproduce the shoaling of the wave dua to decrease of water depth. Both reproduce the nonlinear wave interactions and the harmonics generation. However, there are some differences in the

points closer to the shore, where the second harmonic appears stronger in BOUSS3W than in COULWAVE. Overall it is considered that BOUSS3W behaved quite well considering that it is weakly nonlinear while COULWAVE is fully nonlinear, and so it is expected that differences occur in very shallow waters for these two models.

In future work a more rigorous validation will be performed using the data collected in the scope of the BRISA project, where wave data was collected with several types of equipments.

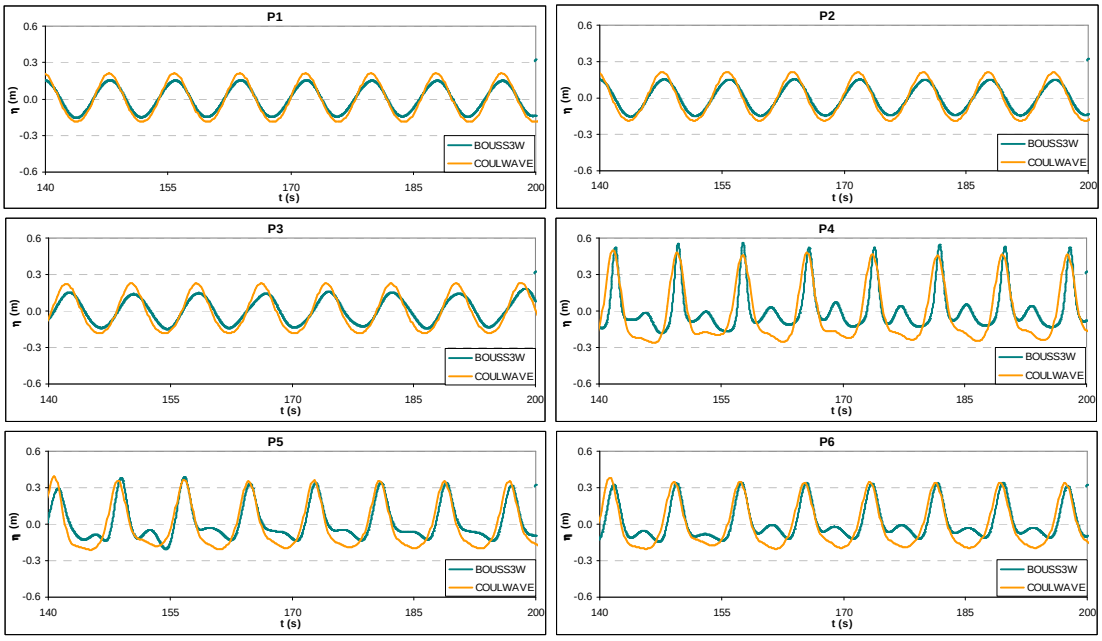

Figure 12: Free surface elevation at points P1 to P6. BOUSS3W (blue), COULWAVE (orange).

5 CONCLUSIONS

This paper described the implementation of bottom friction and wave breaking physical processes in the BOUSS3W model.

Previous applications of the model confirm that the model is able to simulate quite well the main characteristics of the wave field outside and inside harbour configurations. However, neither bottom friction nor wave breaking phenomena were included in the model. These two phenomena constitute an important form of energy dissipation that cannot be neglected in near shore areas.

The bottom friction implementation follows the work of Nwogu and Dermirbilek (2001) .The effect of energy dissipation due to a turbulent bottom boundary layer is simulated by adding a term of bottom shear stress to the momentum equation.

To validate the bottom friction implementation BOUSS3W was run in a simple test case of a flat bottom 2D-Channel. The wave friction factor effect was investigated.

The results showed that:

- The wave energy decreases as the wave propagates consistently with the magnitude of the wave friction factor;
- The bottom friction was adequately implemented in the model;
- The implementation of this new physical phenomenon does not introduce any instability in the model and the viscous damping term was not necessary in any simulation.

After that a real test case was simulated in order to evaluate the model's performance with the new physical phenomenon introduced. Results were compared with another Boussinesq-type model, COULWAVE, Lynett (2002).

The results showed that:

- The model was able to simulate correctly the wave propagation and most of the wave transformations present at Faro beach case;
- In general, both models reproduce well the wave transformations. Both reproduce the shoaling of the wave due to decrease of water depth. Both reproduce the nonlinear wave interactions and the harmonics generation;
- There are some differences in the points closer to the shore, where the second harmonic appears stronger in BOUSS3W than in COULWAVE;
- Overall BOUSS3W behaved quite well considering that it is weakly nonlinear while COULWAVE is fully nonlinear, and so it is expected that differences occur in very shallow waters for these two models.

In future work a more rigorous validation will be performed using the data collected in the scope of the BRISA project, where wave data was collected with several types of equipments. Also the implementation of wave breaking is in validation stage and could not be presented in this work.

ACKNOWLEDGMENTS

The authors would like to acknowledge the financial support from the "Fundação para a Ciência e Tecnologia" (FCT) of the Ministry of Science and Education of Portugal, through projects BRISA PTDC/ECM/67411/2006 and MOIA PTDC/ECM/73145/2006.

REFERENCES

[1] Berzins M., Furzeland R.M., Scales L.E. (1985). *A user's manual for SPRINT -a versatile software package for solving systems of algebraic, ordinary and partial differential equations: Part 3 – advanced use of SPRINT*. Technical Report TNER.85.058, Thornton Res. C, Chester.

[2] Brown P. N., Hindmarsh A.C. And Petzold L.R. (1989). "Using Krylov methods in the solution of large-scale differential-algebraic systems". *SIAM Journal on Scientific Computing*. **15**, 6, pp.1467 - 1488.

[3] Dietrich W. E. (1982) Settling Velocity of Natural Particles. *Water Resources Research*, **Vol. 18**, No. 6, pp1615-1626. December.

[4] Fortes, C.J.E.M.; Silva, L.G.P.; Sousa, I.A. (2005). *Ensaios em modelo reduzido do Porto de Vila do Porto – Santa Maria, Açores*. Relatório 361/05-NPE, LNEC, Novembro. 131pp.

[5] Jimenez J. A. Madsen O.S. (2003) A Simple Formula to Estimate Settling Velocity of Natural Sediments. *Journal of Waterway, Port, Coastal and Ocean Engineering* March/April. 129:2, **70**, pp70-78

[6] Johnson H. K., Kofoed-Hansen H. (2000) Influence of Bottom Friction on Sea Surface Roughness and Its Impact on Shallow Water Wind Wave Modeling. *Journal of physical oceanography.* American Meteorological Society. **Vol 30**. pp 1743-1756.

[7] Kamphuis, J.W. (1975) Friction Factor under Oscillatory Waves. *Journal of the Waterways Harbors and Coastal Engineering Division*, **Vol. 101**, No. 2, May, pp. 135-144.

[8] Lambkin D. *A Review of the Bed Roughness Variable in MIKE 21 FLOW MODEL FM, Hydrodynamic (HD) and Sediment Transport (ST) modules.* Component part of: Dix, J.K., Lambkin, D.O. and Cazenave, P.W. (In preparation) *'Development of a Regional Sediment Mobility Model for Submerged Archaeological Sites'*. University of Southampton, English Heritage ALSF Project No. 5224.

[9] Le Roux, J.P., (2001). A simple method to predict the threshold of particle transport under oscillatory waves. *Sedimentary Geology* **143** (2001): 59–70—Reply to discussion

[10] Nwogu, O. (1993) "Alternative form of Boussinesq equations for near-shore wave propagation". *J. Waterway, Port, Coastal, and Ocean Engineering*. **119**, 6, pp. 618 - 638.

[11] Nwogu, O., Demirbilek, Z. (2001) *BOUSS-2D: A Boussinesq Wave Model for Coastal Regions and Harbors.* Report 1 Theoretical Background and User.s Manual, ERDC/CHL TR-01-25, U.S. Army Corps of Engineers

[12] Pinheiro L., Fortes C.J., Santos J.A., Walkley, M. (2009) Implementation of partial reflection boundary conditions in wave propagation model BOUSS3W. *International Coastal Symposium* ICS 2009. Lisbon.

[13] Pinheiro, L.; Fernandes, J.L.M.; .Fortes, C.J. E.M. (2007a). "Finite Element Mesh Generator with Local Density Conditioned to Bathymetry for Wave Propagation Models in Coastal Zones". *IMACS Series in Comp. and Applied Mathematics, Proc. of EUA4X@IAC 06*, Roma Italy, October 2006. **Vol.12**, pp. 71 - 80.

[14] Pinheiro. L. (2007b). *Um método de elementos finitos para a discretização das equações de Boussinesq estendidas*. Tese de mestrado. Engenharia Mecânica, IST, 105pp.

[15] Raposeiro, P.D.; Fortes, C.J.E.M.; Reis, M.T. (2009) Ferramenta de cálculo e análise do espraiamento em estruturas de enrocamento: caso de estudo Praia de Vale do Lobo. *Proc. 3º Encontro Nacional de Riscos, Segurança e Fiabilidade*, Lisboa, 3 a 5 de Novembro.

[16] Walkley, M. A. (1999). *A Numerical Method for Extended Boussinesq Shallow-Water Wave Equations.* Doctor of Philosophy Thesis. The University of Leeds, School of Computer Studies, Sept., 174pp.

[17] Wei G., Kirby J. T., Sinha A. (1999) "Generation of waves in Boussinesq models using a source function method". *Coastal Engineering*, **36**, pp. 271 – 299.